Int. J. Solids Structures Vol. 15, pp. 427–437
© Pergamon Press Ltd., 1979. Printed in Great Britain

0020-7683/79/0501-0427/$02.00/0

A FINITE ELEMENT APPROACH FOR CABLE PROBLEMS

HALUK OZDEMIR
Earthquake Engineering Systems, Inc., San Francisco, CA 94111, U.S.A.

(*Received* 12 *July* 1978; *received for publication* 10 *October* 1978)

Abstract—A finite element approach is proposed for the static and dynamic nonlinear analysis of cable structures. Starting from the stress equations of equilibrium, a variational formulation is derived in which the static and kinematic variables are measured in some previous configuration of the body. To discretize this variational form of equilibrium equations, Lagrangian functions are employed to interpolate the curved geometry of each element and only displacement continuity is enforced between element nodes. By introducing a separate interpolation for arclength, displacement patterns which leave element nodal arclengths constant are not allowed to induce strains in the element. The finite element matrices resulting from the operations of linearization and discretization are derived. By evaluating the stiffness matrix of the 2-node element, it is shown explicitly that the element stiffness matrix is independent of whether the initial configuration or the current configuration is used in the description of kinematic and static variables. Sample analyses are presented to demonstrate the utility and reliability of the proposed elements.

INTRODUCTION

Because of the high efficiency of steel in simple tension, cable structures provide economical solutions to a wide range of structural engineering problems. For this reason, the analysis of cables has attracted considerable interest in the past and continues to do so at an accelerating rate. Due to their flexibility in bending, cable structures undergo large displacements before attaining their equilibrium configuration. Consequently, it becomes necessary to distinguish between the undeformed and deformed configurations, i.e. the analysis must take into consideration geometric nonlinearity. Analysis for vibrations about a given static equilibrium configuration, however, may be performed using modal superposition if the oscillations are small enough.

Although efforts in analytical treatment of cable problems still continue[1, 2], most of recent research is aimed at dicretizing the equations of equilibrium and solving the resulting nonlinear algebraic equations numerically. Such an approach was used by Leonard and Recker[3], who employed a 2-node finite element to study the dynamic response of lightly stressed cables. The updated formulation implemented in this study did not employ equilibrium iterations, and therefore required linearization of the equations of motion at each step for accurate results. This work was later extended for nonlinear dynamics of curved cables by enforcing continuity of slope across nodal points using approximations to direction cosines[4]. West and Caramanico[5] also derived discrete equations of equilibrium for suspended cables by using 2-node axial elements connected by frictionless pins. Henghold and Russell[6] presented a total Lagrangian formulation for cable structures, employing curved, multinode finite elements. The definition of strain used in this study leads to strains, and therefore stresses, when an initially straight, multinode element assumes a curved shape without changing its arclength between nodal points; it is our opinion that such displacement patterns should not be permitted to induce strains in the element. Gambhir and Batchelor[7] developed a 2-node curved finite element using cubic polynomial interpolation functions and enforcing continuity of nodal displacements and rotations. Their approach is based on shallowness assumptions; therefore, analysis of globally deep cable systems requires a sufficient number of elements to render each element locally shallow.

For the analysis of cable networks, equivalent membrane models have been used extensively. In this relation, the studies of Shore and Bathish[8], Shore and Chaudhari[9], Soler and Afshari[10], Sangster and Batchelor[11] should be mentioned.

In this paper, a finite element approach is presented for the static and dynamic nonlinear analysis of cable structures. Element geometry is interpolated using Lagrangian functions, and only displacement continuity is enforced between element nodes. An independent interpolation is introduced for the arclength in order that displacement patterns which leave arclengths between nodal points constant do not induce strains in the element. The linearization of the nonlinear equations is presented in detail. Because of its simplicity, the 2-node element provides an excellent example in identifying the differences between total and updated Lagrangian formulations; it is shown here that the final stiffness matrix is independent of the choice of reference configuration, although individual matrices leading to the stiffness matrix are different. Finally, example problems are given to demonstrate the utility of the proposed elements.

NOTATION

With regard to subscripts and superscripts, the following convention is employed:

A left superscript denotes the time associated with the configuration in which the quantity occurs. A left subscript denotes the time associated with the reference configuration for the quantity.

A right superscript denotes nodal quantities. A right superscript enclosed in parenthesis indicates that the quantity is associated with an intermediate configuration in the iterative solution scheme. A right subscript denotes the components of a vector or second order tensor; a right subscript following a comma denotes differentiation.

All notation is defined in the next following their first occurence.

VIRTUAL WORK EQUATION FOR A CABLE ELEMENT

Consider the stress equations of equilibrium for a three-dimensional body at time $t+\Delta t$:

$$\frac{\partial}{\partial\,^{t+\Delta t}x_i}(^{t+\Delta t}\sigma_{ij}) + {}^{t+\Delta t}\rho(^{t+\Delta t}b_j - {}^{t+\Delta t}\ddot{x}_j) = 0. \tag{1}$$

Let δu_j be the variations in $^{t+\Delta t}x_j$, assumed consistent with kinematical constraints. Then, multiplying eqn (1) by δu_j and integrating over the volume $^{t+\Delta t}V$ of the body, one obtains

$$\int_{^{t+\Delta t}V} {}^{t+\Delta t}\sigma_{ij} \cdot \frac{1}{2}\left\{\frac{\partial}{\partial\,^{t+\Delta t}x_i}(\delta u_j) + \frac{\partial}{\partial\,^{t+\Delta t}x_j}(\delta u_i)\right\} \mathrm{d}\,^{t+\Delta t}v = {}^{t+\Delta t}R \tag{2}$$

with

$$\begin{aligned} ^{t+\Delta t}R = &\int_{^{t+\Delta t}A} {}^{t+\Delta t}T_j \cdot \delta u_j \,\mathrm{d}\,^{t+\Delta t}a \\ &+ \int_{^{t+\Delta t}V} {}^{t+\Delta t}\rho(^{t+\Delta t}b_j - {}^{t+\Delta t}\ddot{x}_j) \cdot \delta u_j \,\mathrm{d}\,^{t+\Delta t}v \end{aligned} \tag{3}$$

where the first integral in eqn (3) represents the integration of tractions $^{t+\Delta t}T_j$ over the surface area $^{t+\Delta t}A$.

To specialize the virtual work equation for cables, define a cable element to be a structural member characterized by the following idealizations:

1. The element is capable of developing stresses only in the direction of the normal to its cross section.
2. This normal stress is uniform over the cross-sectional area.
3. The cross-sectional area remains constant during deformation.

Thus, only one independent variable, namely arclength, need be used to define the static and kinematic variables at any time.

Using the arclength $^{\bar{t}}s$ associated with the configuration $^{\bar{t}}\chi$ at time $\bar{t}$ as the independent variable eqn (2) can be transformed to read

$$^{t+\Delta t}R = \int_{^{\bar{t}}S} {}^{t+\Delta t}_{\bar{t}}\sigma_{NN} \cdot \delta(^{t+\Delta t}_{\bar{t}}\epsilon_{NN}) A \,\mathrm{d}\,^{\bar{t}}s \tag{4}$$

where A is the cross-sectional area, and $^{t+\Delta t}_{\bar{t}}\sigma_{NN}$, $^{t+\Delta t}_{\bar{t}}\epsilon_{NN}$ denote the (second) Piola–Kirchhoff stress and Green–Lagrange strain at time $t+\Delta t$, referred to the configuration at time $\tilde{t}$:

$$ {}^{t+\Delta t}_{\tilde{t}}\sigma_{NN} = {}^{t+\Delta t}\sigma_{nn}\left(\frac{\mathrm{d}^{\tilde{t}}s}{\mathrm{d}^{t+\Delta t}s}\right) \tag{5} $$

$$ {}^{t+\Delta t}_{\tilde{t}}\epsilon_{NN} = \frac{1}{2}\left\{\left(\frac{\mathrm{d}^{t+\Delta t}s}{\mathrm{d}^{\tilde{t}}s}\right)^2 - 1\right\}. \tag{6} $$

Equation (4) represents the internal virtual work for a cable element in a form that lends itself to linearization about some known configuration of the element; this linearization is the subject of the next section.

LINEARIZATION

To obtain the solution at time $t+\Delta t$, the displacement method will be employed. However, in view of the fact that eqn (4) is nonlinear in displacements, it is necessary to resort to an iterative scheme. The approach used here is to linearize eqn (4) and to solve the resulting equations to obtain an estimate of the solution of the nonlinear problem[12]. This iterative process is repeated until convergence is obtained in some norm.

Let $\mathbf{u}^{(k)}$ denote the kth incremental iterate for the displacements from time t to $t+\Delta t$:

$$ \mathbf{u}^{(k)} = {}^{t+\Delta t}\mathbf{x}^{(k)} - {}^{t+\Delta t}\mathbf{x}^{(k-1)}, \quad k \geq 1, $$

${}^{t+\Delta t}\mathbf{x}^{(0)}$ being some initial estimate of the solution ${}^{t+\Delta t}\mathbf{x}$. Assuming that the constitutive relationship may be linearized to obtain

$$ {}^{t+\Delta t}_{\tilde{t}}\sigma^{(k)} = {}^{t+\Delta t}_{\tilde{t}}\sigma^{(k-1)} + {}^{t+\Delta t}_{\tilde{t}}E^{(k-1)} \cdot \frac{\mathrm{d}}{\mathrm{d}\alpha}\{{}^{t+\Delta t}_{\tilde{t}}\epsilon_{NN}({}^{t+\Delta t}\mathbf{x}^{(k-1)} + \alpha\mathbf{u}^{(k)})\}_{\alpha=0} \tag{7} $$

the linearization of eqn (4) about ${}^{t+\Delta t}\mathbf{x}^{(k-1)}$ is

$$ \begin{aligned} {}^{t+\Delta t}R = &\int_{{}^{\tilde{t}}S} {}^{t+\Delta t}_{\tilde{t}}\sigma^{(k-1)}_{NN} \cdot \frac{\mathrm{d}}{\mathrm{d}\alpha}\{{}^{t+\Delta t}_{\tilde{t}}\epsilon_{NN}({}^{t+\Delta t}\mathbf{x}^{(k-1)} + \alpha \cdot \delta\mathbf{u})\}_{\alpha=0} A\,\mathrm{d}^{\tilde{t}}s \\ &+ \int_{{}^{\tilde{t}}S} {}^{t+\Delta t}_{\tilde{t}}E^{(k-1)} \cdot \frac{\mathrm{d}}{\mathrm{d}\beta}\{{}^{t+\Delta t}_{\tilde{t}}\epsilon_{NN}({}^{t+\Delta t}\mathbf{x}^{(k-1)} + \beta\mathbf{u}^{(k)})\}_{\beta=0} \\ &\cdot \frac{\mathrm{d}}{\mathrm{d}\alpha}\{{}^{t+\Delta t}_{\tilde{t}}\epsilon_{NN}({}^{t+\Delta t}\mathbf{x}^{(k-1)} + \alpha \cdot \delta\mathbf{u})\}_{\alpha=0} A\,\mathrm{d}^{\tilde{t}}s \\ &+ \int_{{}^{\tilde{t}}S} {}^{t+\Delta t}_{\tilde{t}}\sigma^{(k-1)}_{NN} \cdot \frac{\mathrm{d}}{\mathrm{d}\beta}\left(\frac{\mathrm{d}}{\mathrm{d}\alpha}\{{}^{t+\Delta t}_{\tilde{t}}\epsilon_{NN}({}^{t+\Delta t}\mathbf{x}^{(k-1)} + \beta\mathbf{u}^{(k)} + \alpha \cdot \delta\mathbf{u})\}_{\alpha=0}\right)_{\beta=0} A\,\mathrm{d}^{\tilde{t}}s. \end{aligned} \tag{8} $$

Evaluation of the integrals in eqn (8) requires, in general, a knowledge of two configurations of the element (see Fig. 1): the reference configuration ${}^{\tilde{t}}\chi$ in which the independent variables are measured, and the latest known configuration ${}^{t+\Delta t}\chi^{(k-1)}$ about which the equations of equilibrium are linearized. Theoretically, any known configuration of the element may be employed as the reference configuration. From a computational point of view, however, the choice lies essentially between the stress-free configuration ${}^{o}\chi$, and the latest known configuration ${}^{t+\Delta t}\chi^{(k-1)}$. Usually, it is more efficient to take ${}^{o}\chi$ as the reference configuration when the constitutive law takes a simpler form in terms of Piola–Kirchhoff stresses and Green–Lagrange strains; this formulation is called "total Lagrangian"[13, 14]. On the other hand, if the constitutive law is given in terms of Cauchy stresses or Jaumann stress rates and their energy conjugates, the choice of ${}^{t+\Delta t}\chi^{(k-1)}$ as the reference configuration is more effective; in this case, the formulation is called "updated Lagrangian".

The configuration about which the equations are linearized determines the method of solution. If the equations are linearized about the latest known configuration ${}^{t+\Delta t}\chi^{(k-1)}$, as done here, a Newton–Raphson iteration is being implemented. Since formation and triangularization of the structural stiffness matrix entails considerable computation, it is usually more efficient to

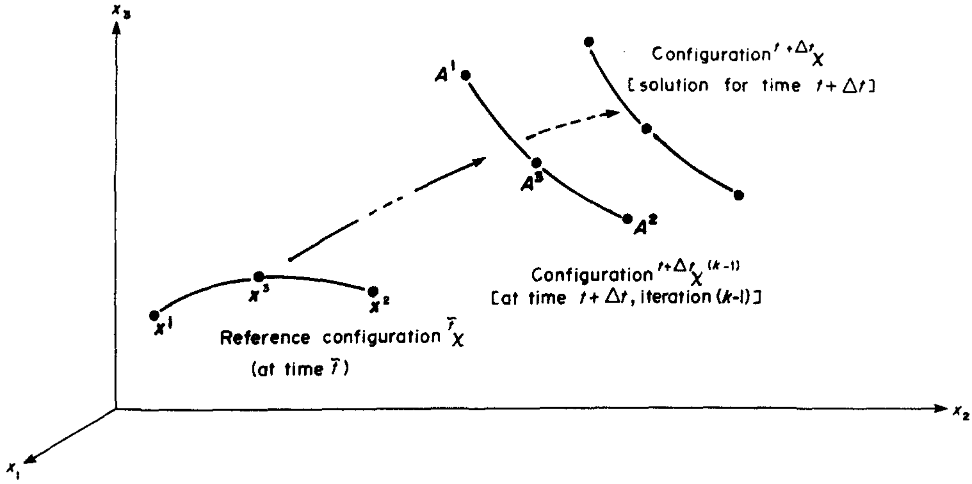

Fig. 1. Motion of cable element.

reform the stiffness matrix only when the solution converges slowly or not at all. In this case, a modified Newton–Raphson method, called constant stiffness iteration, is being employed.

In the next section, eqn (8) is discretized by introducing interpolation for the spatial variables; subsequently, element material and geometric stiffness matrices are derived.

INTERPOLATION FUNCTIONS AND ELEMENT STIFFNESS MATRIX

To obtain the discretized equations of equilibrium, consider an element with nodal coordinates $\mathbf{X}^n$ in the reference configuration $^{\bar{t}}\chi$, where $n = 1, \ldots, N$, and N is the number of nodes. These nodal coordinates are assumed to determine the spatial configuration of the element using

$$^{\bar{t}}\mathbf{x} = \sum_{n=1}^{N} H_n(r)\mathbf{X}^n$$

where the domain of the independent variable r is $[-1, 1]$ and $H_n(r)$ are the Lagrangian interpolation functions with equally-spaced nodal points.

Let $\mathbf{A}^n$ denote the coordinates of the element in the configuration about which the equations are to be linearized, namely $^{t+\Delta t}\chi^{(k-1)}$, and let $\mathbf{U}^n$ denote the incremental nodal displacements for the kth iteration. Then

$$^{t+\Delta t}\mathbf{x}^{(k-1)} = \sum H_n\mathbf{A}^n$$

$$\mathbf{u}^{(k)} = {}^{t+\Delta t}\mathbf{x}^{(k)} - {}^{t+\Delta t}\mathbf{x}^{(k-1)} = \sum H_n\mathbf{U}^n.$$

A "consistent" interpolation for the arclength would thus be given by

$$^{t+\Delta t}s^{(k-1)}(r) = \int_{-1}^{r} \{({}^{t+\Delta t}\mathbf{x}_{,r}^{(k-1)})^T({}^{t+\Delta t}\mathbf{x}_{,r}^{(k-1)})\}^{1/2}\,\mathrm{d}r.$$

To show that this interpolation for the arclength is not desirable for a cable, consider a 3-node element which, in its reference configuration, lies along the x_1-axis:

$$\mathbf{X}^1 = \begin{bmatrix} 0 \\ 0 \\ 0 \end{bmatrix}, \quad \mathbf{X}^2 = \begin{bmatrix} {}^{\bar{t}}L \\ 0 \\ 0 \end{bmatrix}, \quad \mathbf{X}^3 = \begin{bmatrix} \frac{1}{2}{}^{\bar{t}}L \\ 0 \\ 0 \end{bmatrix}$$

where $^{\bar{t}}L$ is the length, and $\mathbf{X}^3$ denotes the coordinates of the midnode. Assume that during the course of deformation, the element takes a parabolic shape in the x_1–x_2 plane without any change between nodal arclengths:

$$\mathbf{A}^1 = \begin{bmatrix} 0 \\ 0 \\ 0 \end{bmatrix}, \quad \mathbf{A}^2 = \begin{bmatrix} 1 \\ 0 \\ 0 \end{bmatrix}, \quad \mathbf{A}^3 = \begin{bmatrix} \frac{1}{2} \\ \frac{1}{4} \\ 0 \end{bmatrix}$$

with

$$ {}^{t}s\big|_{r=0} = {}^{t+\Delta t}s\big|_{r=0} = \tfrac{1}{2}{}^{t}L$$
$$ {}^{t}s\big|_{r=1} = {}^{t+\Delta t}s\big|_{r=1} = {}^{t}L.$$

Therefore, by eqn (6), the Green–Lagrange strain at any point r is

$${}^{t+\Delta t}_{\ t}\epsilon(r) = \frac{1}{2}\left\{\frac{1+r^2}{{}^{t}L} - 1\right\} \neq 0.$$

Since the configuration ${}^{t+\Delta t}\chi$ should not be considered a strain inducing state with reference to ${}^{t}\chi$, it is necessary to introduce an an alternate interpolation for the arclength. This is accomplished here by using Lagrangian interpolation functions:

$$\left.\begin{aligned} {}^{t}s(r) &= \sum^{N} H_n(r)\,{}^{t}S^n \\ {}^{t+\Delta t}s^{(k-1)}(r) &= \sum^{N} H_n(r)\,{}^{t+\Delta t}S^n \end{aligned}\right\} \tag{9}$$

$$\left.\begin{aligned} {}^{t}S^n &= \int_{-1}^{r_n} \{({}^{t}\mathbf{x}_{,r})^T({}^{t}\mathbf{x}_{,r})\}^{1/2}\,\mathrm{d}r \\ {}^{t+\Delta t}S^n &= \int_{-1}^{r_n} \{({}^{t+\Delta t}\mathbf{x}^{(k-1)}_{,r})^T({}^{t+\Delta t}\mathbf{x}^{(k-1)}_{,r})\}^{1/2}\,\mathrm{d}r. \end{aligned}\right\} \tag{10}$$

With these definitions, displacement patterns which leave nodal arclengths ${}^{t}S^n$ constant do not induce strains in the element. Such displacement patterns include, but are not limited to, rigid body translations and rotations.

Matrices ${}^{t+\Delta t}_{\ t}\mathbf{B}_M$ and ${}^{t+\Delta t}_{\ t}\mathbf{B}_G$ are defined by

$${}^{t+\Delta t}_{\ t}\mathbf{B}_M\delta\mathbf{U} = \frac{\mathrm{d}}{\mathrm{d}\alpha}\{{}^{t+\Delta t}_{\ t}\epsilon_{NN}({}^{t+\Delta t}\mathbf{x} + \alpha\cdot\delta\mathbf{u})\}_{\alpha=0}$$

$$\delta\mathbf{U}^T({}^{t+\Delta t}_{\ t}\mathbf{B}_G)\mathbf{U} = \frac{\mathrm{d}}{\mathrm{d}\beta}\left(\frac{\mathrm{d}}{\mathrm{d}\alpha}\{{}^{t+\Delta t}_{\ t}\epsilon_{NN}({}^{t+\Delta t}\mathbf{x} + \beta\cdot\mathbf{u} + \alpha\cdot\delta\mathbf{u})\}_{\alpha=0}\right)_{\beta=0}$$

with dimensions $(1\times 3N)$ and $(3N\times 3N)$, respectively. Using the notation

$$\mathbf{H} = (H_1\mathbf{I}|H_2\mathbf{I}|\cdots|H_N\mathbf{I})$$

$$h_n = \frac{\mathrm{d}}{\mathrm{d}r}H_n$$

$$\mathbf{h} = \frac{\mathrm{d}}{\mathrm{d}r}\mathbf{H},$$

$${}^{t+\Delta t}D = \{({}^{t+\Delta t}\mathbf{x}_{,r})^T({}^{t+\Delta t}\mathbf{x}_{,r})\}^{1/2},$$

where $\mathbf{I}$ is the (3×3) identity matrix, one obtains

$${}^{t+\Delta t}_{\ t}\mathbf{B}_M = \left(\frac{\mathrm{d}^{t+\Delta t}s}{\mathrm{d}^{t}s}\right)\cdot\left(\frac{\mathrm{d}r}{\mathrm{d}^{t}s}\right)\cdot\left\{\sum^{N} h_n \int_{-1}^{r_n} \frac{1}{{}^{t+\Delta t}D}\,{}^{t+\Delta t}\mathbf{x}^T_{,r}\mathbf{h}\,\mathrm{d}r\right\} \tag{11}$$

$$ {}^{t+\Delta t}_{\ t}\mathbf{B}_G = \left(\frac{\mathrm{d}^{t+\Delta t}s}{\mathrm{d}^t s}\right)\cdot\left(\frac{\mathrm{d}r}{\mathrm{d}^t s}\right)\cdot\left\{\sum^N h_n \int_{-1}^{r_n} \frac{1}{{}^{t+\Delta t}D} h^T\left(\mathbf{I} - \frac{{}^{t+\Delta t}\mathbf{x}_{,r}}{{}^{t+\Delta t}D}\frac{{}^{t+\Delta t}\mathbf{x}_{,r}^T}{{}^{t+\Delta t}D}\right)\mathbf{h}\,\mathrm{d}r\right\} $$

$$ + \left(\frac{\mathrm{d}^t s}{\mathrm{d}^{t+\Delta t}s}{}^{t+\Delta t}_{\ t}\mathbf{B}_M\right)^T\left(\frac{\mathrm{d}^t s}{\mathrm{d}^{t+\Delta t}s}{}^{t+\Delta t}_{\ t}\mathbf{B}_M\right). \tag{12} $$

Referring to eqn (8), the material and geometric stiffness matrices are thus given by

$$ {}^{t+\Delta t}\mathbf{K}_M = \int_{{}^t S} {}^{t+\Delta t}_{\ t}\mathbf{B}_M{}^T \cdot (A^{t+\Delta t}_{\ t}E)\cdot {}^{t+\Delta t}_{\ t}\mathbf{B}_M\,\mathrm{d}^t s \tag{13} $$

$$ {}^{t+\Delta t}\mathbf{K}_G = \int_{{}^t S} ({}^{t+\Delta t}_{\ t}\sigma_{NN}A)^{t+\Delta t}_{\ t}\mathbf{B}_G\,\mathrm{d}^t s. \tag{14} $$

The equivalent nodal force vector ${}^{t+\Delta t}\mathbf{F}$ is also calculated via the ${}^{t+\Delta t}_{\ t}\mathbf{B}_M$ matrix:

$$ {}^{t+\Delta t}\mathbf{F} = \int_{{}^t S} ({}^{t+\Delta t}_{\ t}\sigma_{NN}A)^{t+\Delta t}_{\ t}\mathbf{B}_M{}^T\,\mathrm{d}^t s. $$

In general, the evaluation of the stiffness matrix and nodal forces requires numerical integration. For the 2-node element, however, the integrands are constant and the integrals are easily calculated, as shown in the next section.

STIFFNESS MATRIX FOR 2-NODE ELEMENT

In this section, explicit expressions are derived for the stiffness of a 2-node element. It is shown that the total and updated Lagrangian formulations do in fact lead to identical matrices, verifying that different formulations may be employed for different elements in a structure. The results obtained here are also compared with previously published results.

Let ${}^tL$ denote the length of the element at time t, and define direction cosines as follows;

$$ {}^{t+\Delta t}\mathbf{a} = \frac{{}^{t+\Delta t}\mathbf{A}^2 - {}^{t+\Delta t}\mathbf{A}^1}{{}^{t+\Delta t}L} $$

$$ {}^{t+\Delta t}\mathbf{c} = ({}^{t+\Delta t}\mathbf{a})({}^{t+\Delta t}\mathbf{a}^T) $$

$$ {}^{t+\Delta t}\mathbf{C} = \begin{bmatrix} {}^{t+\Delta t}\mathbf{c} & -({}^{t+\Delta t}\mathbf{c}) \\ -({}^{t+\Delta t}\mathbf{c}) & {}^{t+\Delta t}\mathbf{c} \end{bmatrix}. $$

Then, eqns (11) and (12) give

$$ {}^{t+\Delta t}_{\ t}\mathbf{B}_M = \left(\frac{{}^{t+\Delta t}L}{{}^tL}\right)^2\left(\frac{1}{{}^{t+\Delta t}L}\right)\langle -({}^{t+\Delta t}\mathbf{a})^T, {}^{t+\Delta t}\mathbf{a}^T\rangle $$

$$ {}^{t+\Delta t}_{\ t}\mathbf{B}_G = \left(\frac{1}{{}^tL}\right)^2\begin{bmatrix} \mathbf{I} & -\mathbf{I} \\ -\mathbf{I} & \mathbf{I} \end{bmatrix}. $$

Therefore, the stiffness matrix ${}^{t+\Delta t}\mathbf{K}$ is

$$ \begin{aligned} {}^{t+\Delta t}\mathbf{K} &= {}^{t+\Delta t}\mathbf{K}_M + {}^{t+\Delta t}\mathbf{K}_G \\ &= \frac{A^{t+\Delta t}_{\ t}E}{{}^{t+\Delta t}L}\left(\frac{{}^{t+\Delta t}L}{{}^tL}\right)^3 {}^{t+\Delta t}\mathbf{C} + \left(\frac{{}^{t+\Delta t}_{\ t}P}{{}^tL}\right)\begin{bmatrix} \mathbf{I} & -\mathbf{I} \\ -\mathbf{I} & \mathbf{I} \end{bmatrix}. \end{aligned} \tag{15} $$

It should be noted that the above stiffness matrix is general in the sense that no specific constitutive equation has been employed in its derivation. Assume now that the Piola–Kirchhoff stress ${}^{t+\Delta t}_{\ o}\sigma_{NN}$ is linear in the Green–Lagrange strain ${}^{t+\Delta t}_{\ o}\epsilon_{NN}$, both referred to the stress-free configuration ${}^o\chi$:

$$ {}^{t+\Delta t}_{\ o}\sigma_{NN} = E^{t+\Delta t}_{\ o}\epsilon_{NN}. \tag{16} $$

The stiffness matrix is then given by

$$^{t+\Delta t}\mathbf{K}=\frac{AE}{^{t+\Delta t}L}\left(\frac{^{t+\Delta t}L}{^{o}L}\right)^{3}{}^{t+\Delta t}\mathbf{C}+\frac{^{t+\Delta t}_{\ \ o}P}{^{o}L}\begin{bmatrix}\mathbf{I} & -\mathbf{I}\\ -\mathbf{I} & \mathbf{I}\end{bmatrix}. \tag{17}$$

The significance of this equation lies in the fact that none of the quantities appearing in it are referred to the configuration $^{\bar{t}}\chi$; in other words, the stiffness matrix is independent of the choice of reference configuration. To further illustrate this point, assume that $^{\bar{t}}\chi$ coincides with $^{t+\Delta t}\chi$; i.e. implement an updated Lagrangian formulation. Then eqn (15) gives

$$^{t+\Delta t}\mathbf{K}=\frac{A^{t+\Delta t}_{t+\Delta t}E}{^{t+\Delta t}L}{}^{t+\Delta t}\mathbf{C}+\frac{^{t+\Delta t}_{t+\Delta t}P}{^{t+\Delta t}L}\begin{bmatrix}\mathbf{I} & -\mathbf{I}\\ -\mathbf{I} & \mathbf{I}\end{bmatrix}.$$

Substituting for $^{t+\Delta t}_{t+\Delta t}E$ and $^{t+\Delta t}_{t+\Delta t}P$ in terms of E and $^{t+\Delta t}{}_{o}P$, one again obtains eqn (17).

A commonly used constitutive law relates Cauchy stress to change in length:

$$^{t+\Delta t}\sigma_{nn}=E\left(\frac{^{t+\Delta t}L-{}^{o}L}{^{o}L}\right). \tag{18}$$

In this case, the stiffness matrix is obtained as

$$^{t+\Delta t}\mathbf{K}=\frac{AE}{^{t+\Delta t}L}{}^{t+\Delta t}\mathbf{C}+\frac{^{t+\Delta t}_{t+\Delta t}P}{^{t+\Delta t}L}\begin{bmatrix}\mathbf{I} & -\mathbf{I}\\ -\mathbf{I} & \mathbf{I}\end{bmatrix}. \tag{19}$$

An alternative approach for the derivation of the stiffness matrix of a 2-node element consists of expressing equilibrium directly in terms of nodal forces. The stiffness matrix is then obtained by taking derivatives with respect to incremental displacements. This approach has been used in Ref. [15] for the constitutive relationship of eqn (18); the resulting matrix agrees with eqn (19). Differences between the matrices obtained here and those in Refs. [16] and [17] are due to different definitions of strain for the large displacement case. The total Lagrangian formulation of Ref. [6], on the other hand, does lead to the same stiffness matrix as given in eqn (17) for the constitutive relationship of eqn (16).

EXAMPLE PROBLEMS

In order to demonstrate the reliability and utility of the finite element presented here, three example problems which have been published previously were solved. In all examples, the constitutive relationship of eqn (16) was assumed valid; compared to eqn (18), this law renders the material stiffness matrix stiffer in tension and more flexible in compression. For frequency and dynamic response calculations, the consistent mass matrix was employed exclusively.

As the first example, the fundamental frequency of the (2×2) cablenet of Fig. 2 was calculated. When the deadload is not taken into consideration, the first mode involves only out of plane displacements so that the fundamental frequency is determined solely by the geometric stiffness matrix. Frequencies calculated with and without the deadload were, in fact, found to be identical as the additional stresses induced in the elements are very small compared to the initial stress. The frequencies obtained here along with previously published results are given in Table 1, where it is evident that the present method does provide an excellent alternative.

The second example involves calculation of in-plane frequencies of the single span cable of Fig. 3, in equilibrium under its deadload. Using the nondimensional "stiffness/weight" parameter AE/mgL introduced in Ref. [6], where mgL is the total weight, frequencies were obtained for $AE/mgL = 1000$.

Table 2 gives the results obtained by modelling the cable using 8 elements. It is observed that the frequencies decrease monotonically as the number of element nodes increase; moreover, as in the previous example, the 3-node element mesh gives results very close to that of the 4-node mesh. In Table 3 frequencies obtained by using different number of 3-node elements are tabulated; in this case, a monotonic convergence is not observed for each

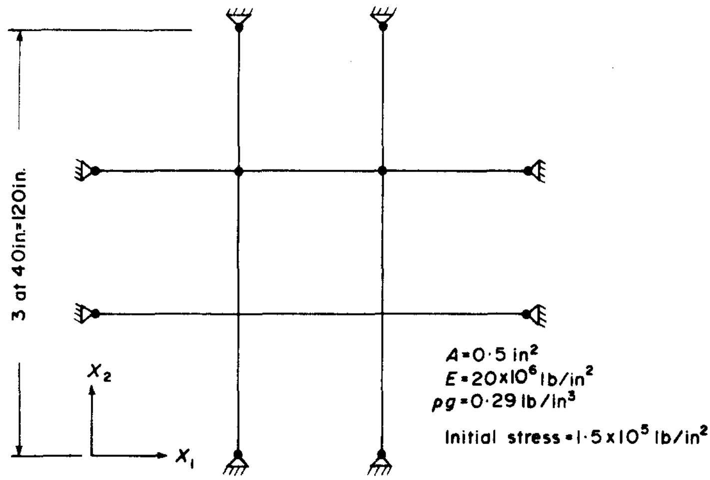

Fig. 2. (2 × 2) Flat orthogonal cablenet.

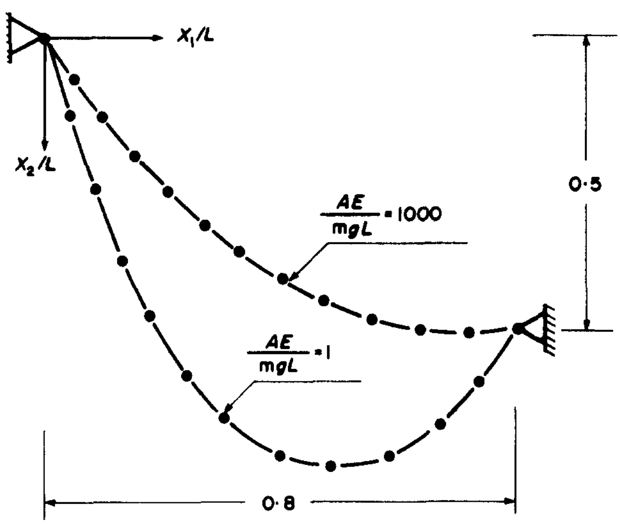

Fig. 3. Equilibrium configuration of single span cables.

Table 1. Comparison of fundamental frequency (Hz) of 2 × 2 cablenet obtained by various methods

Method of analysis	Frequency (Hz)
Soler and Afshari[10]	59.10
Shore and Chaudhari[9]	
1. Lumped mass analysis	56.40
2. Membrane analysis	58.80
Sangster and Batchelor[11]	
1. Lumped mass analysis	56.76
2. Equivalent membrane analysis	60.43
Leonard[4]	
1. (3 × 3) grid	61.59
2. (6 × 6) grid	59.55
3. (12 × 12) grid	59.05
Gambhir and Batchelor[7]	60.06
Present method	
(12 elements, consistent mass)	
1. 2-node elements	61.64
2. 3-node elements	58.97
3. 4-node elements	58.93

Table 2. Frequencies (Hz) of single span cable obtained by using 8 elements ($AE/mgL = 1000$)

Mode	2-Node elements	3-Node elements	4-Node elements
1	4.418	4.337	4.336
2	7.107	6.756	6.750
3	10.32	9.441	9.409
4	13.49	11.85	11.76

Table 3. Frequencies (Hz) of single span cable obtained by using 3-node elements ($AE/mgL = 1000$)

	2 Elements		4 Elements		6 Elements		8 Elements	
Mode	Present method	Ref. [6]	Present method	Ref. [6]	Present method	Ref. [6]	Present method	Ref. [6]
1	4.318	11.397	4.346	4.611	4.338	4.457	4.337	4.404
2	8.102	15.470	6.776	7.962	6.768	7.229	6.756	7.001
3	32.43	—	9.599	—	9.496	—	9.441	—
4	95.97	—	13.02	—	11.86	—	11.85	—

frequency. Comparison of results with those of Ref. [6] shows that, for crude meshes, the elements proposed here will provide better results. For finer meshes, the frequencies obtained here are slightly lower, as shown in Table 3.

The last problem considered is the dynamic response of an initially stressed straight cable subjected to uniform transverse load. Cable dimensions and material properties are given in Fig. 4. Using twelve 3-node elements, the fundamental frequency of the cable in its initial configuration is calculated to be 0.2506 Hz, which is in exact agreement with the classical result $f = \frac{1}{2}(T/\rho AL^2)^{1/2}$, T being the prestressing force. Under deadload, the displacement of the cable at the center is $w = 131.6$ in.; its fundamental frequency then increases to 0.3852 Hz. Variation of w under increasing uniform transverse load, applied staticly, is shown in Fig. 5, where hardening of the system is clearly displayed. The dynamic response of the cable when

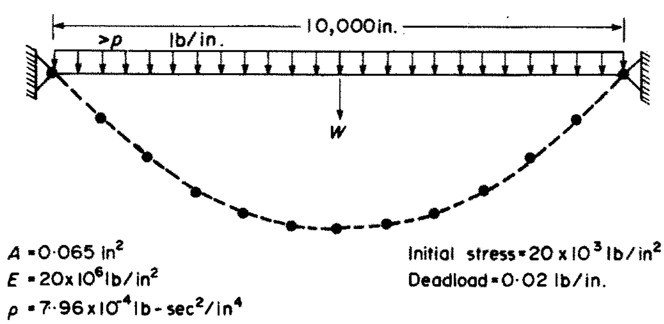

Fig. 4. Single span, straight cable.

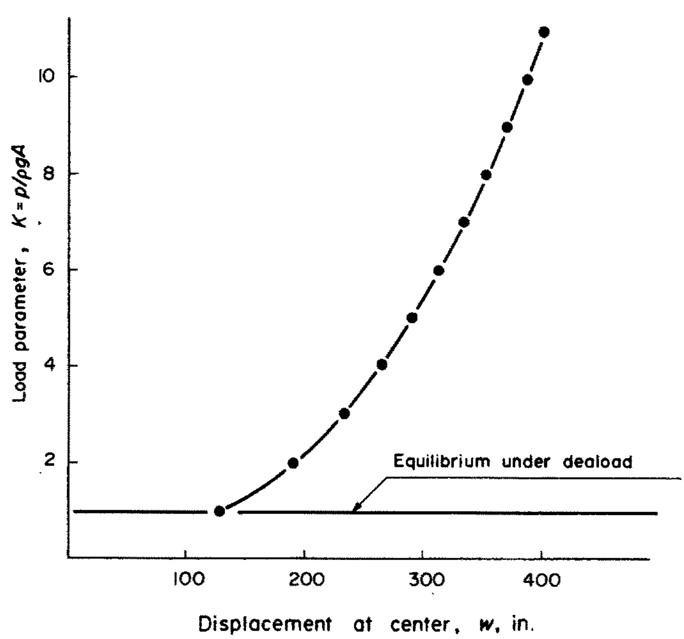

Fig. 5. Displacement of straight cable under uniformly distributed static loading.

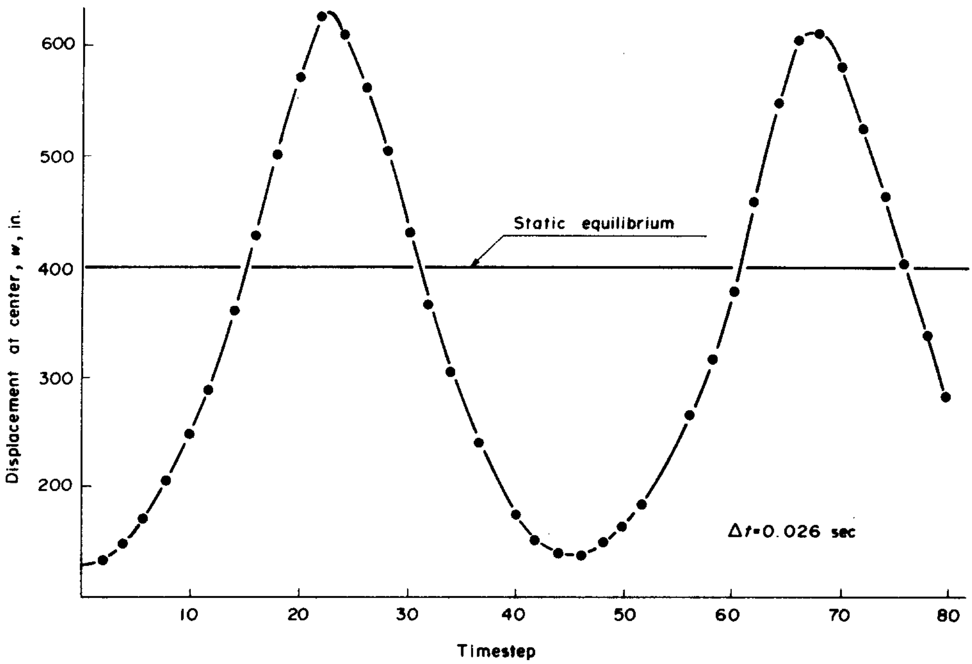

Fig. 6. Dynamic response of straight cable under uniformly distributed, suddenly applied loading.

subjected to a suddenly applied uniform load of $p = 2$ lb/in. is plotted in Fig. 6. In comparing these results with those of Ref. [3], it is seen that the present formulation leads to a stiffer system. Under deadload, the displacement of the center node is reported to be approximately 190 in., about 50% higher than the present result. Under dynamic loading, the first peak displacement obtained here is 616 in., compared to 660 in. given in Ref. [3].

CONCLUDING REMARKS

A new family of three-dimensional curved finite elements has been presented for the analysis of cable structures. The derivation is based on the assumption that element behavior is governed by one-dimensional normal stress; thus, these elements may be used in modelling other uniaxial members such as reinforcing rods.

The spatial configuration of an N-node element is interpolated using an $(N-1)$st degree polynomial; therefore, cables that are initially curved or cables that assume a curved shape as a result of deformation can be modelled very accurately by using multinode elements.

The development of the linearized equilibrium equations has been verified by comparing the 2-node element stiffness matrix with previously published results. Theoretically, the element stiffness matrix is independent of the reference configuration; it has been explicitly shown here for the 2-node element that the stiffness matrices obtained by using different reference configurations are, in fact, identical.

The example problems verify that the 3-node element does provide a refined analysis capability for a wide range of cable problems.

REFERENCES

1. H. H. West and A. R. Robinson, Continuous method of suspension bridge analysis. *J. Struct. Div., Proc. ASCE* **94** (1968).
2. H. M. Irvine and T. K. Caughey, The linear theory of free vibrations of a suspended cable. *Proc. R. Soc. (London)* **A341** (1974).
3. J. W. Leonard and W. W. Recker, Nonlinear dynamics of cables with initial tension. *J. Engng Mech. Div., Proc. ASCE* **98** (1972).
4. J. W. Leonard, Dynamics of curved cable elements. *J. Engng Mech. Div., Proc. ASCE* **99** (1973).
5. H. H. West and D. L. Caramanico, Initial-value discrete suspension bridge analysis. *Int. J. Solids Structures* **9** (1973).
6. W. M. Henghold and J. J. Russell, Equilibrium and natural frequencies of cable structures (a nonlinear finite element approach). *Comput. Structures* **6** (1976).
7. M. L. Gambhir and B. Batchelor, A finite element for 3-D prestressed cablenets. *Int. J. Num. Meth. Engng* **11** (1977).
8. S. Shore and G. N. Bathish, Membrane analysis of cable roofs. In *Space Structures* (Edited by R. M. Davies). Blackwell, Oxford (1967).

9. S. Shore and B. Chaudhari, Free vibrations of cable networks utilizing analogous membrane. *Proc. Int. Assoc. Bridges Structural Engng., 9th Congress*, Amsterdam (1972).
10. A. I. Soler and H. Afshari, On the analysis of cable network vibrations using Galerkin method. *J. Appl. Mech., Proc. ASME* 37 (1970).
11. K. G. Sangster and B. Batchelor, Nonlinear dynamic analysis of 3-D cablenets, Computational Methods in Nonlinear Mechanics. *Proc. Int. Conf. Computat. Meth. Nonlinear Mech.*, University of Texas at Austin (1974).
12. C Lanczos, *The Variational Principles of Mechanics*, 4th Edn. University of Toronto Press, Toronto, Canada (1970).
13. K. J. Bathe and H. Ozdemir, Elastic–plastic large deformation static and dynamic analysis. *Comput. Structures* 6 (1976).
14. K. J. Bathe, H. Ozdemir and E. L. Wilson, Static and dynamic, geometric and material nonlinear analysis. *Rep. No: UC SESM* 74-4, University of California, Berkeley, Structural Engng Lab., Berkeley (1974).
15. M. J. Turner, E. H. Dill, H. C. Martin and R. J. Melosh, Large deflection of structures subjected to heating and external loads. *J. Aerospace Sci.* 27 (1960).
16. H. C. Martin, On the derivation of stiffness matrices for the analysis of large deflection and stability problems, *Proc. Conf. Matrix Meth. Struct. Engng.* Wright-Patterson AFB, Ohio (1966).
17. J. A. Stricklin, W. E. Haisler and W. A. Von Riesemann, Geometrically nonlinear structural analysis by direct stiffness method. *J. Struct. Div., Proc. ASCE* 97 (1971).